Journal of Machine Engineering, 2019, Vol. 19, No. 2, 54–62
ISSN 1895-7595 (Print) ISSN 2391-8071 (Online)

Received: *26 February 2019* / Accepted: *10 May 2019* / Published online: *29 June 2019*

hard machining, CBN tool,
tool wear, specific energy

Wit GRZESIK[1]
Berend DENKENA[2]
Krzysztof ZAK[1*]

ENERGY-BASED CHARACTERIZATION OF PRECISION HARD MACHINING USING PARTIALLY WORN CBN CUTTING TOOLS

This paper highlights the performance of precision hard turning with CBN cutting tools from energy point-of-view with additional tool wear effect. For this purpose several wear tests were performed during which the tool nose wear VB_C and the corresponding changes of component forces F_c, F_f and F_p were continuously measured. Based on the measured forces and geometrical characteristic of the uncut layer, specific cutting and ploughing energy were determined for several combinations of cutting parameters. Consequently, changes of energy consumption resulting from tool wear evolution for variable feed rate, depth of cut and tool nose radius were presented.

1. INTRODUCTION

Hard machining is one of leading finishing processes used in the mass production of geared shafts, bearing and hydraulic components made of hardened steels, which replaces or assists grinding operations [1, 2]. Unfortunately, the main drawbacks which reduce the efficiency of dry machining of hard materials include such technological problems as excessive tool wear and shorter tool life, unsatisfactory surface integrity and dimensional and shape part accuracy [3–5]. Moreover, hard machining consumes more energy not only due to high material hardness (even above 60 HRC) but also results from the specific action of the chamfered cutting edge. In addition, excessive tool wear intensifies friction and ploughing action of the cutting edge. For instance [6] the coefficient of sliding friction can increase even above 3 due to the presence of high-temperature adhesion which increases rapidly during tool wear. The machining technological system should be very stiff because the radial (passive) force is substantially higher in comparison to conventional turning of softer materials. Consequently, the radial force influences both static and dynamic behaviour of the machining system. This effect becomes important when tool wear progresses, especially when using CBN cutting tools with large nose radius of 0.8 and

[1] Faculty of Mechanical Engineering, Opole University of Technology, Poland
[2] Gottfried Wilhelm Leibniz Universität Hannover, Germany
E_mail: k.zak@po.opole.pl
https://doi.org/10.5604/01.3001.0013.2223

1.2 mm [7]. The motivation for a deeper analysis of the energy balance in PHT operations was that it has not yet been investigated in a satisfactory manner for the machining practice.

It was practically confirmed [8] that machining of hardened materials with CBN chamfered tools produces substantially higher passive forces resulting in more intensive ploughing action, which, in turn, causes higher friction and wear, and lower tool life. In addition, tool nose radius changes uncut chip geometry which intensifies ploughing effect in the hard turning process [9]. This study analysis the energy output in the precision hard turning of 16MnCrS5 (AISI 5115) hardened steel with worn CBN tools under the variable feed rate, the depth of cut and tool nose radius. The input data includes the component forces F_c, F_f and F_p measured continuously during tool wear period [7]. The obtained values of the specific cutting energy resulting from both tool wear and changes of the process variables were mapped in the loge_c-logh_m graph and compare with other machining operations [10].

2. MECHANICS OF THE MACHINING PROCESS

2.1. GEOMETRY OF CROSS-SECTIONAL AREA OF CUT

It is well documented that in finish turning with round-cornered tools the depth of cut (a_p) is generally smaller than the tool nose radius (r_ε) and the cross-sectional area of cut has a comma shape as shown in Fig. 1a [13]. For such cut geometry, the cutting ratio b/h is higher than 1. The cross-section area is determined as the product of the effective contact length l_k and the average uncut chip thickness (UCT) h_m (see Eqn. 4). This assumption is based on the replacing of a curvilinear cutting edge by an equivalent straight cutting edge (ECE) which is oriented by the effective tool edge angle κ_{re} as shown in Fig. 1b.

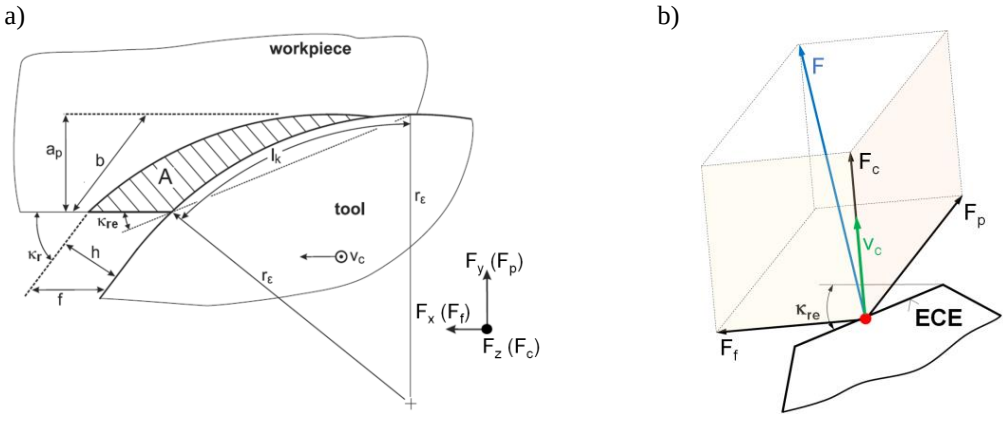

Fig. 1. Dimensioning of the cross-section area (a) and equivalent cutting edge – ECE (b), [11]

Cutting tool angles and dimensions of the cross-cut layer shown in Fig. 1a (the cutting tool angle κ_{re}, the contact length l_k, the average UCT h_m, the area of cut A_{nc}) are determined using a set of equations (1–4) appropriately.

$$\kappa_{re} = \frac{1}{2}\arccos\left(\frac{r_\varepsilon - a_p}{r_\varepsilon}\right) \quad (1)$$

$$l_k = 2\kappa_{re} r_\varepsilon \quad (2)$$

$$h_m = a_p f / l_k \quad (3)$$

$$A_{nc} = l_k h_m \quad (4)$$

2.2. DETERMINATION CUTTING FORCES AND SPECIFIC ENERGIES

In this study, three components of the resultant cutting force (F_x, F_y and F_z) were measured in the *xyz* coordinate system shown in Fig. 1b. Based on the measured values of the force components specific cutting e_c and ploughing e_p energies were determined using Eqns. 5 and 6 respectively. Hence

$$e_c = F_c / A_{nc} \quad (5)$$

$$e_p = F_p / A_{nc} \quad (6)$$

3. EXPERIMENTAL DETAILS

This study is based on the data obtained in finish hard turning of a case-hardened 16MnCrS5 (AISI 5115) steel with the average micro-hardness of 850-800 $HV_{0.05}$. The machining tests were performed on a CNC lathe Gildemeister CTX 520 linear using CBN cutting tools, grade WBN 560 by *CeramTec*, with 56% CBN content and an average grain size of 3 μm. The following cutting tool angles were specified: the effective rake angle $\gamma_{ne} = -24°$, the chamfer angle $\gamma_{fe} = -30°$,the clearance angle $\alpha_n = 6°$ and the inclination angle $\lambda_s = -6°$. The cutting edge radius was assumed to be equal to $r_\beta = 8$ μm.

Table 1. Sets of cutting conditions used in this study

No. set of cutting parameters	Tool nose radius, r_ε, mm	Feed rate, f, mm/rev	Depth of cut, a_p, mm
1	0.1	0.1	0.1
2	0.4		
3	0.8		
4	1.2		
5	0.8	0.1	0.01
6			0.1
7			0.2
8	0.8	0.01	0.1
9		0.1	
10		0.2	

The combinations of machining parameters are specified in Table 1. They include three variable values of feed rate (f = 0.01, 0.1 and 0.2 mm/rev), depth of cut (a_p = 0.01, 0.1 and 0.2 mm) and four tool nose radiuses (r_ε = 0.1, 0.4, 0.8 and 1.2 mm). All turning tests

were performed with constant cutting speed of 150 m/min. It can be noted, based on Eqns. 1–3, that due to changes of the feed, the depth of cut and tool corner radius the effective tool edge angle κ_{re} and the average uncut chip thickness h_m vary substantially. The values of the effective tool edge angle κ_{re} computed by Eqn. 1 vary from 5° for the minimum value of a_p = 0.01 mm (r_ε = 0.1 mm, f = 0.1 mm/rev) to 45° for the minimum value of r_ε = 0.1 mm, (f = 0.1 mm/rev, a_p = 0.1 mm). The corresponding values of the average uncut chip thickness h_m computed by Eqn. 3 are presented in Fig. 2a–c. As shown in Fig. 2 its value changes from about 2.5 μm for the minimum feed of 0.01 mm/rev up to about 65 μm for the minimum corner radius of 0.1 mm.

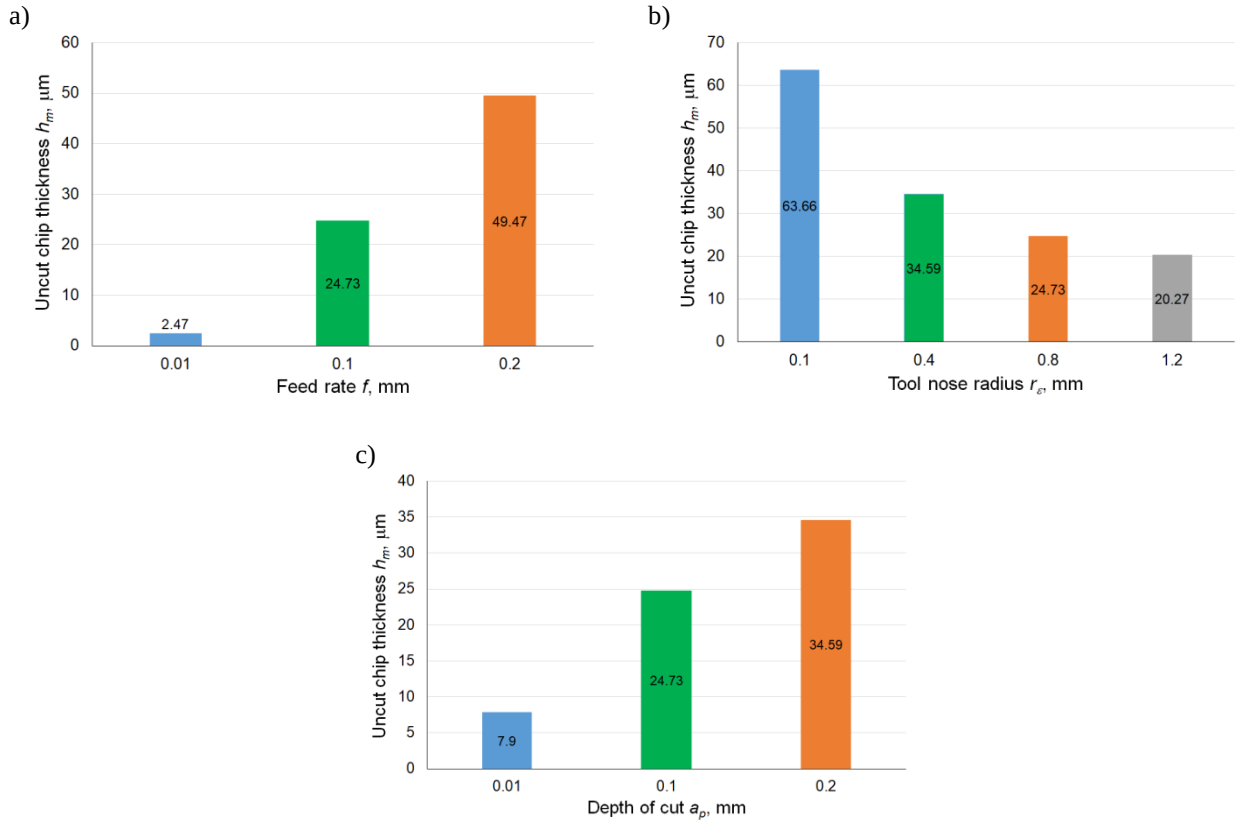

Fig. 2. Changes of average UCT (h_m) for variable feed (a), corner radius (b) and depth of cut (c)

All these geometrical modifications of the UCT cause that the three components F_z, F_y and F_x (equivalently F_c, F_f and F_p forces) the resultant cutting force F change according to the resolution scheme shown in Fig. 1b. They were measured using a three-component piezoelectric dynamometer Kistler – model 9121. In particular, the recorded force signals were processed with a sampling rate of f = 1 kHz and a low-pass filter with a cut-off frequency of f_c = 300 Hz [7]. The tool wear threshold was assumed to be equal to the tool corner indicator $VB_C \approx 200$ μm [7, 13]. Using the methodology described in Chapter 2, the changes of specific energies during all 7 sets of wear tests (Table 1) were determined (sets No. 3, 6 and 9 are repeated). The input data (values of force components and relevant tool wear indicators) were adopted from [7, 11].

4. RESULTS AND DISCUSSION

4.1. CHANGES OF FORCE COMPONENTS WITH TOOL WEAR

Fig. 3 shows an exemplary case of evolutions of force components measured along with tool wear for variable feed rate and keeping the depth of cut at 0.1 mm and the tool corner radius at 0.8 mm. It is evident in Fig. 3c that the passive force F_p is the dominant force component and its value increases visibly independently of feed rate employed. For instance, for the minimum feed of 0.01 mm/rev the F_p force rises during test time from about 30 N for fresh cutting tools to about 80 N for worn tools.

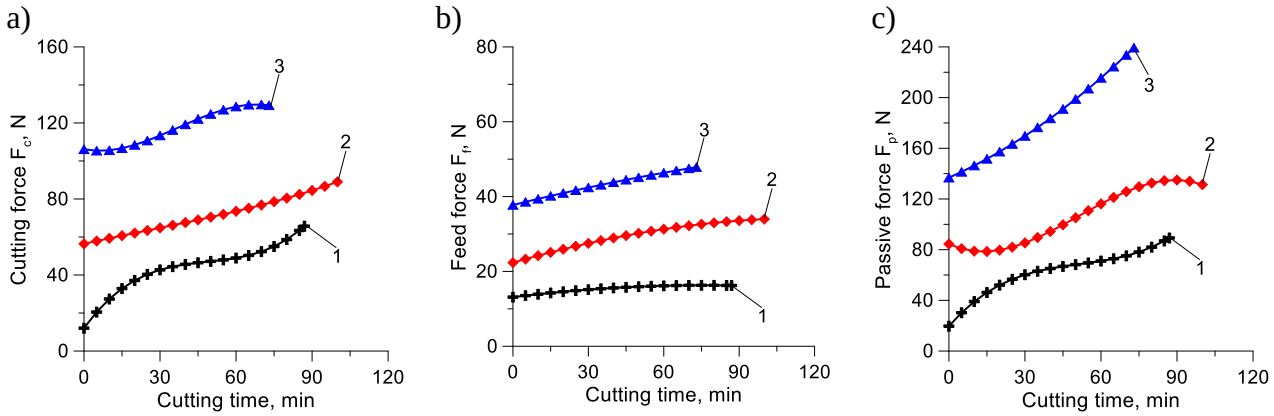

Fig. 3. Changes of force components for variable feed rate: a) F_c; b) F_f; c) F_p resulting from tool wear progressing. Feed rate: 1 – 0.01 mm, 2 – 0.1 mm, 3 – 0.2 mm, constant cutting parameters: a_p = 0.1 μm, r_ε = 0.8 μm

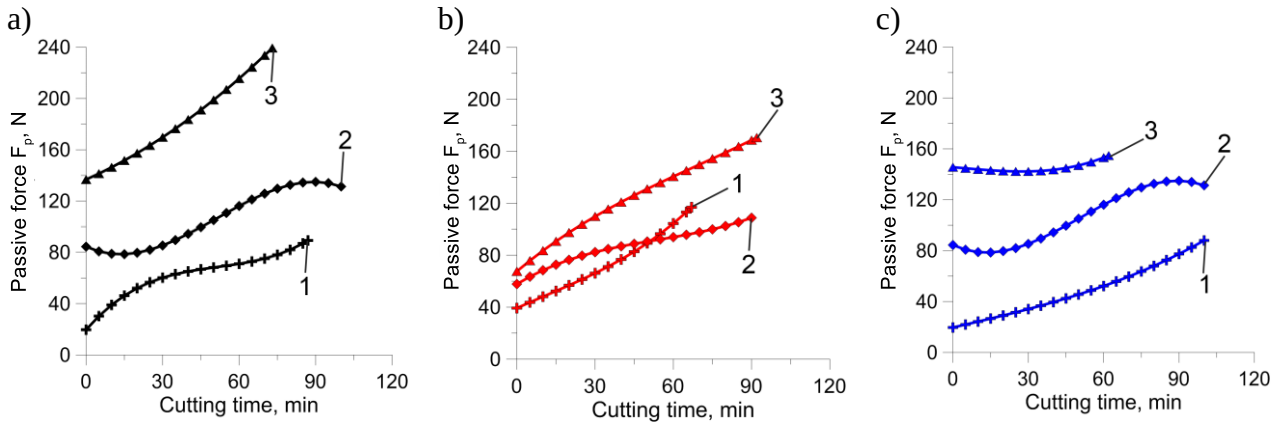

Fig. 4. Changes of passive force F_p for: a) variable feed: 1 – 0.01 mm, 2 – 0.1 mm, 3 – 0.2 mm; b) variable corner radius: 1 – 0.1 mm, 2 – 0.4 mm, 3 – 1.2 mm; c) variable depth of cut: 1 – 0.01 mm, 2 – 0.1 mm, 3 – 0.2 mm

Similar effect was revealed for the cutting force F_c (Fig. 3a). It is noticeable that the changes of cutting force F_c (Fig. 3b) is substantially less intensive than feed force F_f.

In general, according to graphs presented in Fig. 4, the highest increment of the F_p force was observed for the maximum feed rate of 0.2 mm/rev (Fig. 4a), the maximum

corner radius of 1.2 mm (Fig. 4b) and the minimum depth of cut of 0.01 mm (Fig. 4c). An excessive rise of the F_c and F_f forces during tool wear was observed for the lowest corner radius of 0.1 mm [7].

4.2. CHANGES OF SPECIFIC ENERGY COMPONENTS DURING TOOL WEAR

In this study the evolution of tool wear was characterized in terms of associated changes the specific cutting energy (e_c) and the ploughing energy (e_p) consumed. The specific cutting energy represents the energy required to remove the unit volume of material depending on the value of the cutting force F_c whereas the specific ploughing energy represents the friction losses resulting from the action of the passive force F_p.

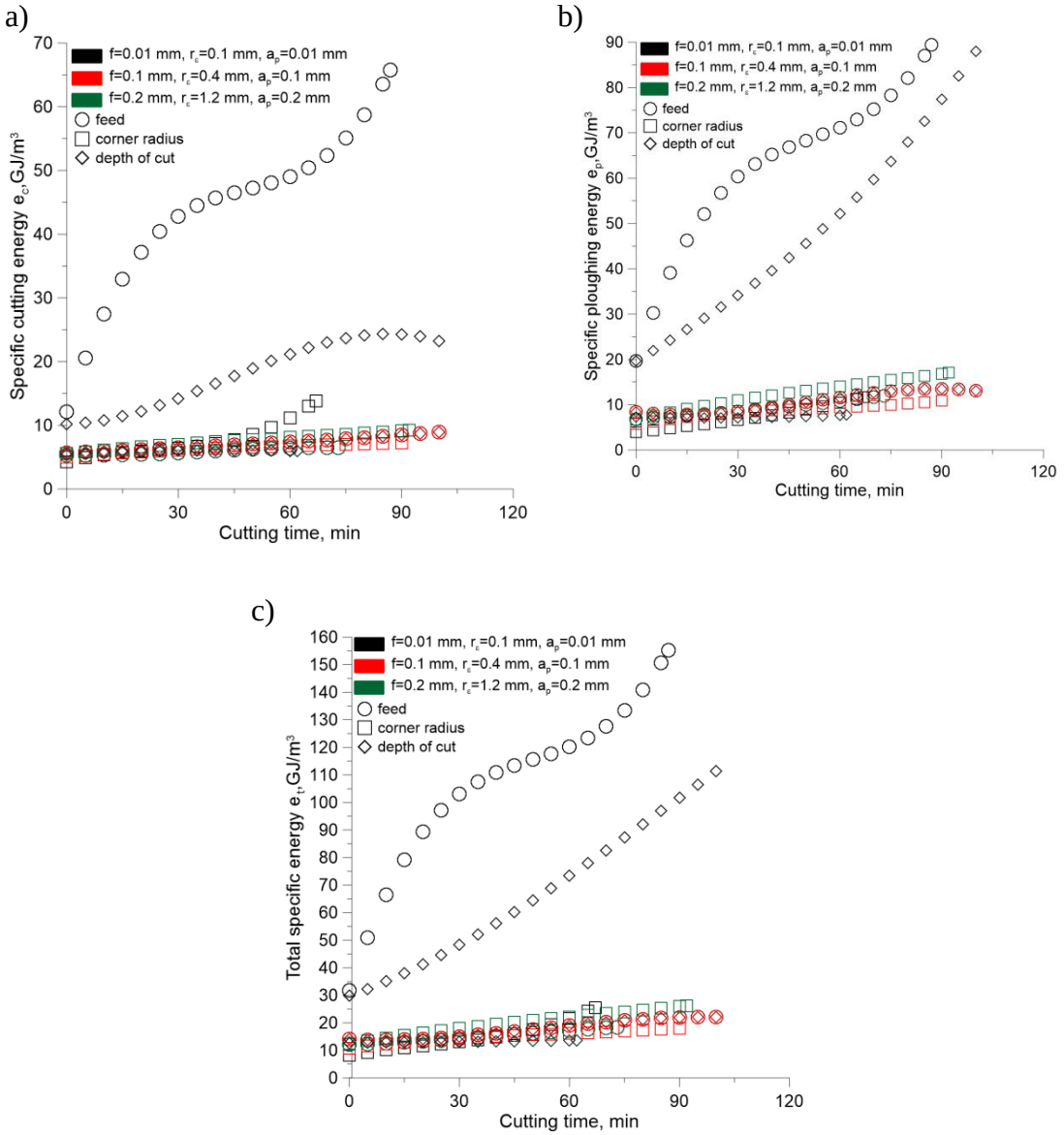

Fig. 5. Comparison of energy balance for different hard machining conditions used in this study: a) specific cutting, b) ploughing energy, c) total energy

Fig. 5 shows the changes of the total specific energy (Fig. 5c) and its components energy (Figs. 5a and 5b respectively) corresponding to tool wear evolution using variable feed rate, depth of cut and tool nose radius. In particular, Fig. 5b indicates that the highest value of specific ploughing energy $e_p \approx 90$ GJ/m^3 corresponds to the lowest feed $f = 0.01$ mm/rev and the lowest depth of cut $a_p = 0.01$ mm at the end of tool wear test.

Changes of the components of specific energy and total specific energy as functions of the feed rate, nose radius and the depth of cut are presented in Figs. 5a and 5b, and 5c respectively. It was revealed that tool wear contributes mostly to the changes of specific ploughing energy rather than the specific cutting energy (Fig. 5b vs. Fig. 5a).

An important finding is that the energy consumed for ploughing action of the tool over the hard surface predominantly overestimates the cutting energy (typically the ratio e_c/e_p is lower than 1 and ranges between 0.5 and 0.8). However, two specific cases can be distinguished in Figs. 5a and 5b. The first when the ratio e_c/e_p oscillates around 1 was observed for the smallest nose radius of 0.1 mm and the second when the e_c/e_p decreases down to the minimum value of about 0.26 is characteristic for the lowest depth of cut of 0.01 mm. In other words, the specific ploughing energy is about four times higher than the specific cutting energy (88 GJ/m^3 *vs.* 23.3 GJ/m^3). As a result, the total specific energy determined as the sum of the e_c and e_p increases rapidly during tool wear for the minimum feed of 0.01 mm/rev up to about 160 GJ/m^3 as shown in Fig. 5a. Less intensive increase of the e_t value is observed for the lowest depth of cut of 10 μm for which the maximum et value approaches 110 GJ/m^3. For other cases presented in Fig. 4c the et value does not exceed 30 GJ/m^3. This energy amount is characteristic for steel grinding with extremely low uncut chip thickness of 2 μm or lower [10, 14].

4.3. MAPPING OF ENERGY DISTRIBUTION FOR DIFFERENT CHIP GEOMETRY

Fig. 6 shows the map which compares specific cutting and total energies for different hard CBN turning operations and their evolution during tool wear. These are $\log e_t - \log h_m$ graphs which highlight how the undeformed chip thickness influences the values of e_c and e_t for different machining parameters and tool corner radius. It should be noted that two data sets denoted by symbols 4 and 5 and 6 and 7 correspond to the tool corner radius of 0.8 mm ($h_m = 24.7$ μm) and 0.4 mm ($h_m = 34.6$ μm) respectively. On the other hand, the maximum UCT of 63.7 μm corresponds to the minimum corner radius of $r_\varepsilon = 0.1$ mm (bar #9).

In Fig. 6a a line corresponding to both grinding and conventional cutting operations of alloy steels are marked in order to compare energy consumptions in hard and conventional (soft) turning operations. The boundary between grinding and cutting operations was selected at the UCT of 20 μm. It is interesting that for medium UCT values ranging from 20 μm to 50 μm the values of the specific cutting energy related to the beginning of tool wear are lower than for conventional turning operations. However, an intensive ploughing action in hard machining causes that the total specific energy which aggregates both cutting and friction interactions exceeds substantially the specific energy in conventional machining (Fig. 6b).

As discussed in Section 4.2 due to extremely small UCT in the range of several microns the values of energy consumed when machining with the lowest feed rate of 0.01 mm/rev and the lowest depth of cut of 0.01 mm (Fig. 5a) are typical for finish grinding of alloy steels, as presented in [10, 14]. In these cases the minimum UCT is equal to 2.5 μm and 7.9 μm respectively (Fig. 2). It is interesting to note in Fig. 6 that a visible increase of e_t during tool wear is also obtained when the tool corner is equal r_ε = 0.1 mm which corresponds to the maximum value of h_{min} of about 64 μm (bar #9).

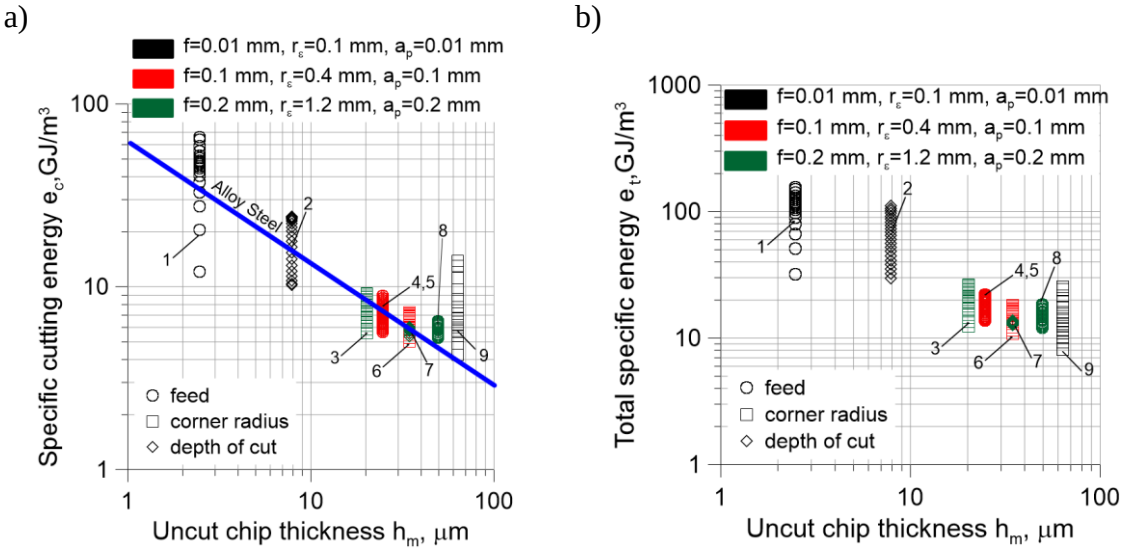

Fig. 6. The dependence of cutting (a) and total (b) specific energy on uncut chip thickness h_m: 1 – 2.5 μm, 2 – 7.9 μm, 3 – 20.3 μm, 4,5 – 24.7 μm, 6,7 – 34.6 μm, 8 – 49.5 μm, 9 – 63.7 μm. Cutting parameters: 1 – f = 0.010 mm/rev, 2 – a_p = 0.01 mm, 3 – r_ε = 1.2 mm, 4 – f = 0.1 mm, 5 – a_p = 0.1 mm, 6 – r_ε = 0.4 mm, 7 – a_p = 0.2 mm, 8 – f = 0.2 mm, 9 – r_ε = 0.1 mm

5. CONCLUSIONS

The following conclusions can be drawn based on the obtained results and their analysis:

- The first specific feature of CBN precision hard turning is that the ploughing energy is generally higher than cutting energy. An exceptional case when the e_c/e_p ratio is about 1 concerns turning operations using CBN tools with small nose radius.
- The second specific feature of CBN PHT with lower feed rate and depth of cut can be compared to grinding with extremely low UCT of about 2 μm. In contrast, the hard turning with higher feed rate and depth of cut is comparable to conventional turning of carbon and alloy steels with the UCT higher than 20 μm.
- From the practical point of view, the ratio of the specific cutting to ploughing energy (e_c/e_p) seems to be an important optimize criterion for hard machining operations.
- Next practical sounds from this study is that the energy consumption in finishing hard turning operations can be reduced when selected low feed rates and depths of cut, and larger tool nose radii.

REFERENCES

[1] GRZESIK W., 2011, *Mechanics of Cutting and Chip Formation*, Chapter 3 in DAVIM J.P, Machining of Hard Materials, Springer, London, 87–114.
[2] BYRNE G., DORNFELD D., DENKENA D., 2003, *Advancing cutting technology*, CIRP Annals, 52/2, 483–507.
[3] TÖNSHOFF H.K., ARENDT C., BEN AMOR R., 2000, *Cutting of hardened steel*, CIRP Annals, 49/2, 547–566.
[4] DAVIES M.A., CHOU Y., EVANS C.J., 1996, *On chip morphology, tool wear and cutting mechanics*, CIRP Annals, 45/1, 77–82.
[5] CHINCHANIKAR S., CHOUDHURY S.K., 2015, *Machining of hardened steel – Experimental investigations, performance modelling and cooling techniques*, A review, Int. J. Mach. Tool Manuf., 89, 95–109.
[6] PANDIT S.M., KASHOU S., 1983, *Variation in friction coefficient with tool wear*, Wear, 84, 65–79.
[7] MAYER R., KÖHLER J., DENKENA B., 2012, *Influence of the tool corner radius on the tool wear and process forces during hard turn*ing, Int. J. Adv. Manuf. Technol., 58, 933–940.
[8] ZHOU J.M., WALTER H., ANDERSSON M., STAHL J.E., 2003, *Effect of chamfer angle on wear of PCBN cutting tool*, Int. J. Mach. Tool Manuf. 43, 301–305.
[9] CHOU Y.K., SONG H., 2014, *Tool nose radius effect on finish hard turning*, J. Mat. Proc. Technol., 148, 259–268.
[10] BOOTHROYD G., KNIGHT W.A., 2005, *Fundamentals of machining and machine tools*, Taylor & Francis, New York.
[11] GRZESIK W., DENKENA B., ŻAK K., GROVE T., BERGMAN B., 2016, *Energy consumption characterization in precision hard machining using CBN cutting tool*, Int. J. Adv. Manuf. Technol., 85/9–12, 2839–2845.
[12] GRZESIK W., DENKENA B., ŻAK K., GROVE T., BERGMAN B., 2015 *Correlation between friction and wear of cubic boron nitride cutting tools in precision hard machinin*g, J. Manuf. Sci. Eng., 138/3, doi: 10.1115/ 1.4031189.
[13] GRZESIK W., 2017, *Advanced machining processes of metallic materials*, Elsevier, Amsterdam.
[14] GRZESIK W., ŻAK K., CHUDY R., 2017, *Influence of tool nose radius on the cutting performance and surface finish during hard turning with CBN cutting tools*, Journal of Machine Engineering. 17/2, 56–64.